

Supplement of “Isotope diffusion in ice enhanced by vein-water flow”

by Felix S. L. Ng

- 5 Movies S1–S3: Here, captions only. Access the movies via doi:10.15131/shef.data.21805803
Please use <https://figshare.com/s/79e62bdae0f84a2efa11> during the review stage.

Figs. S1–S3

- 10 **Movie S1.** Influence of the vein-water flow velocity w on the pattern of δ in the ice–vein system and on the amount of excess
diffusion at $T = -32$ °C, for a signal with wavelength $\lambda = 0.02$ m. These simulations show how the isotopic “shear layer”
described in Sect. 3 evolves and transitions between the sheet regime and tail regime as w changes in small steps from -50 m
 yr^{-1} to 50 m yr^{-1} and back, for the model parameters $a = 1$ μm , $b = 1$ mm and $\alpha = 1$. (a) δ -variations at the vein (red curve)
and in the grain interior at $r = b$ (black curve). (b) Colour map of the pattern of δ in the ice. (c) The corresponding decay-rate
15 enhancement factor f (white dot), located on the surface of $f(\lambda, w)$ in Fig. 7a.

Movie S2. Influence of vein-water flow velocity w on the pattern of δ in the ice–vein system and on the amount of excess
diffusion at $T = -32$ °C, for a signal with wavelength $\lambda = 0.08$ m. The simulation scheme and layout of panels are the same as
in Movie S1.

- Movie S3.** Compressional scaling of the surfaces of (a) signal decay-rate enhancement factor f , (b) $\log_{10}f$ and (c) signal
20 migration velocity v , over the λ – w parameter space, as temperature decreases from -20 °C to -60 °C. Some axis ranges are
updated at -35 °C and -47 °C to focus on relevant variations.

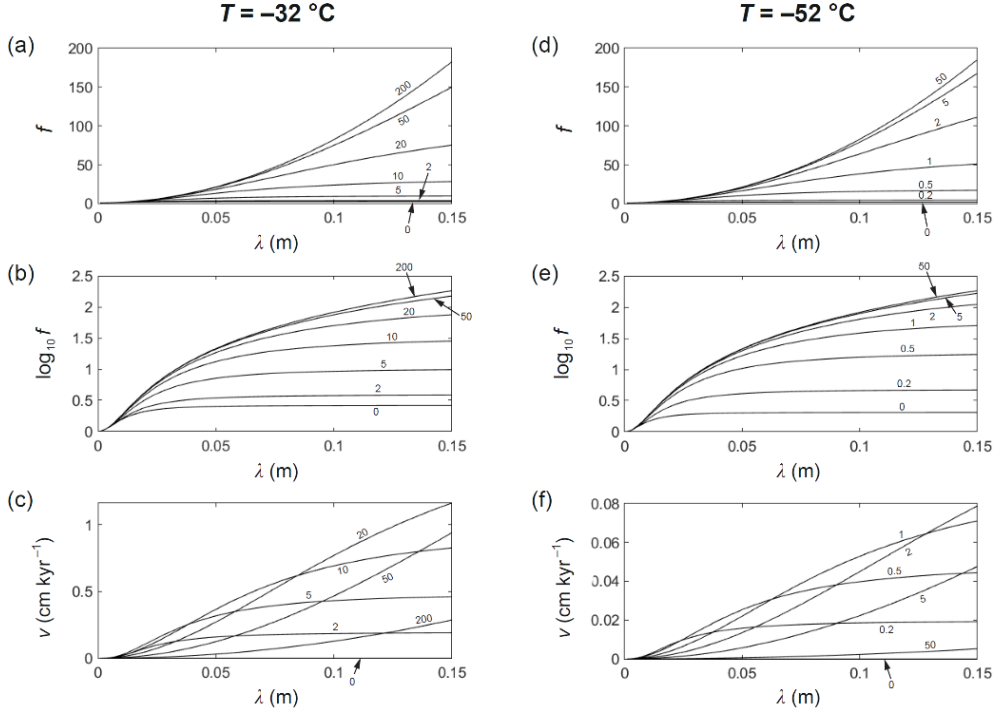


Figure S1. Computed curves of signal decay-rate enhancement factor f , $\log_{10} f$ and signal migration velocity v versus signal wavelength λ , at (a–c) $T = -32\text{ }^{\circ}\text{C}$ and (d–f) $T = -52\text{ }^{\circ}\text{C}$, for different vein-water flow velocities w (curve labels in m yr^{-1}) and assuming the deuterium–hydrogen fractionation coefficient, $\alpha = 1.021$. These curves differ negligibly from those in Fig. 6, where $\alpha = 1$ is assumed. Results based on the ^{18}O – ^{16}O fractionation coefficient, $\alpha = 1.0029$, are still closer to those in Fig. 6.

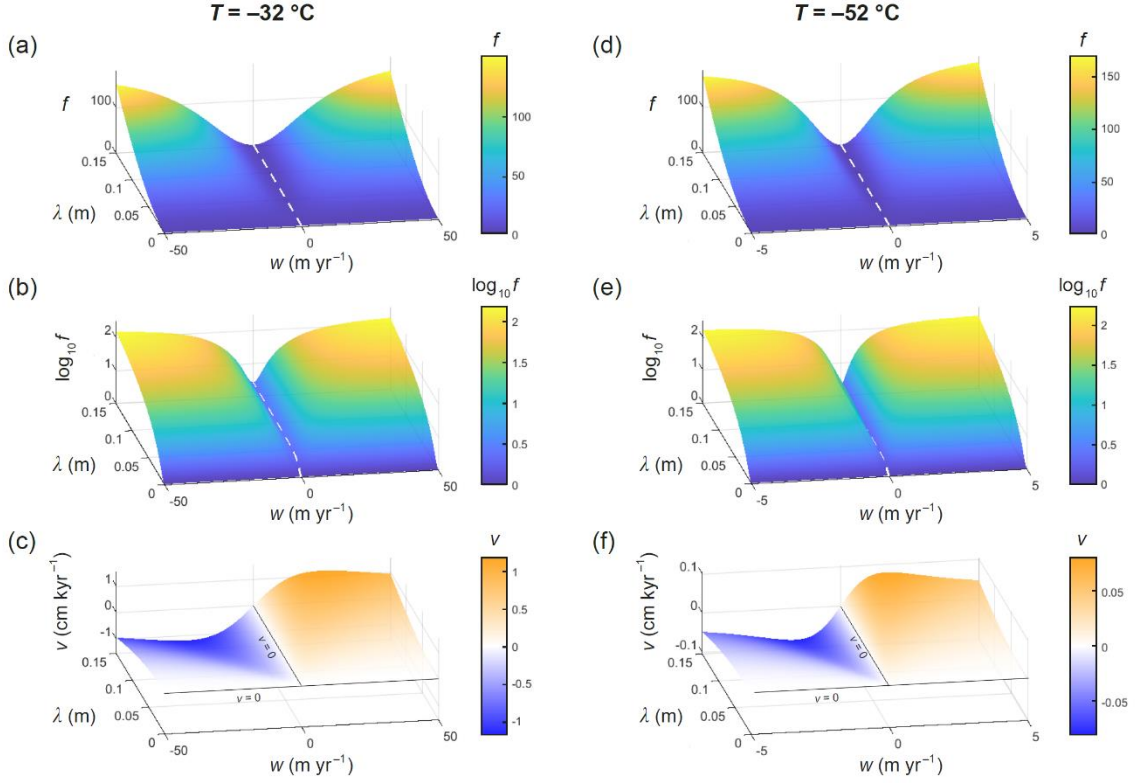
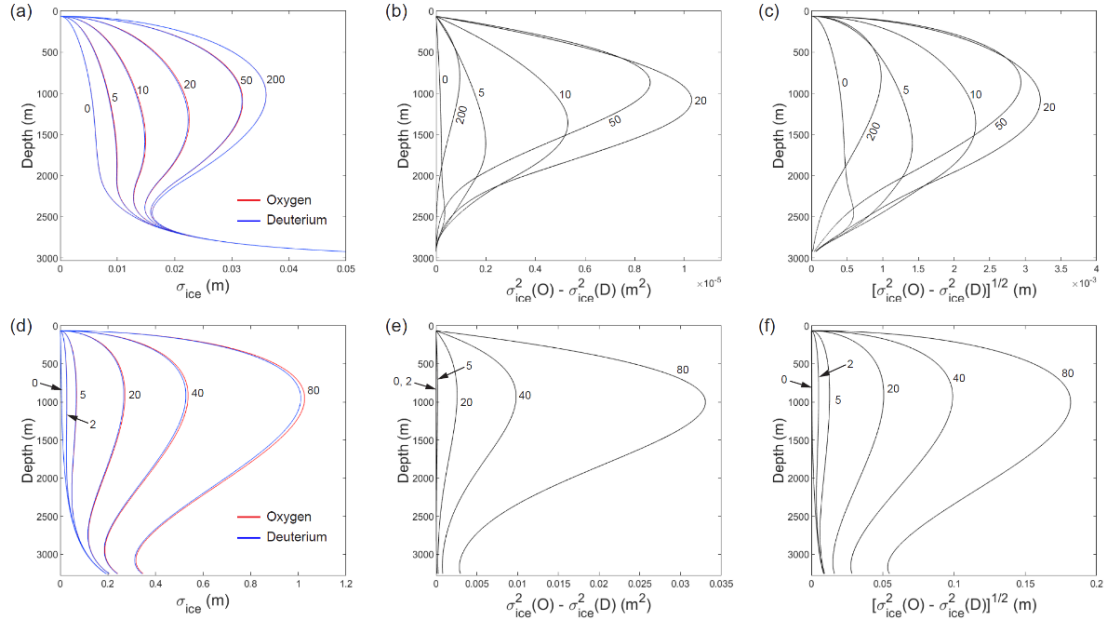


Figure S2. Surfaces of the signal decay-rate enhancement factor f , $\log_{10} f$ and signal migration velocity v over the λ - w parameter space, computed for (a-c) $T = -32$ °C and (d-f) $T = -52$ °C and assuming the deuterium-hydrogen fractionation coefficient, $\alpha = 1.021$. These surfaces differ negligibly from those in Fig. 7, where $\alpha = 1$ is assumed. Results based on the

45 ^{18}O - ^{16}O fractionation coefficient, $\alpha = 1.0029$, are still closer to those in Fig. 7.

GRIP



EPICA

Figure S3. A study of the ice contribution to the differential diffusion length at the (a–c) GRIP and (d–f) EPICA ice-core sites, in model runs using constant grain radius $b = 2$ mm and different vein-water flow velocities w (curve labels in m yr^{-1}). Depth profiles of (a, d) the ice diffusion lengths $\sigma_{\text{ice}}(\text{O})$ and $\sigma_{\text{ice}}(\text{D})$, (b, e) the square differential $\Delta\sigma_{\text{ice}}^2 = \sigma_{\text{ice}}^2(\text{O}) - \sigma_{\text{ice}}^2(\text{D})$, and (c, f) the differential $\Delta\sigma_{\text{ice}}$.